Effect of Posture Change on the Geometric Features of the Healthy Carotid Bifurcation

Nicolas Aristokleous, Ioannis Seimenis, Yannis Papaharilaou, Georgios C. Georgiou, Brigitta C. Brott, Eleni Eracleous, and Andreas S. Anayiotos

***Abstract*—Segmented cross-sectional MRI images were used to construct 3-D virtual models of the carotid bifurcation in ten healthy volunteers. Geometric features, such as bifurcation angle, internal carotid artery (ICA) angle, planarity angle, asymmetry angle, tortuosity, curvature, bifurcation area ratio, ICA/common carotid artery (CCA), external carotid artery (ECA)/CCA, and ECA/ICA diameter ratios, were calculated for both carotids in two head postures: 1) the supine neutral position; and 2) the prone sleeping position with head rotation to the right ($\sim 80^\circ$). The results obtained have shown that head rotation causes 1) significant variations in bifurcation angle [32% mean increase for the right carotid (RC) and 21% mean decrease for the left carotid (LC)] and internal carotid artery angle (97% mean increase for the RC, 43% mean decrease for the LC); 2) a slight increase in planarity and asymmetry angles for both RC and LC; 3) minor and variable curvature changes for the CCA and for the branches; 4) slight tortuosity changes for the braches but not for the CCA; and 5) unsubstantial alterations in area and diameter ratios (percentage changes $<10\%$). The significant geometric changes observed in most subjects with head posture may also cause significant changes in bifurcation hemodynamics and warrant future investigation of the hemodynamic parameters related to the development of atherosclerotic disease such as low oscillating wall shear stress and particle residence times.**

***Index Terms*—Carotid bifurcation, image-based CFD, medical imaging, posture changes.**

I. Introduction

STROKE is the third leading cause of death in the United States resulting in 137 119 deaths in 2006, and accounts for approximately 795 000 cases each year, 610 000 of which are first attacks [1]. Asymptomatic carotid stenosis presents a significant risk factor for stroke with a prevalence of 2–8% [2], while symptomatic patients have statistically significant higher rates of stroke compared to asymptomatic cohort [3]. Several studies over the years have demonstrated that the geometry of the carotid bifurcation predicts blood flow patterns and have postulated that it directly influences the formation of atherosclerotic plaques [3]–[5]. Since even subtle changes in geometry can have a strong influence on the blood flow field, it has been proposed that the individual's vascular geometry may be related to the risk of arterial disease [6].

Recent reports [7] highlight the fact that peripheral arteries in parts of the body that undergo motion and posture change, such as the carotid, femoral, and popliteal arteries, may experience changes in geometry and subsequently in hemodynamics. The influence of posture change on the geometry and hemodynamics of the carotid bifurcation has not been thoroughly studied. Such changes may alter the hemodynamic variables that are generally associated with the development of atherosclerosis, such as low oscillating wall shear stress (WSS) and particle residence times. Using ultrasound imaging, Glor *et al.* have first reported that head rotation may cause geometric changes to the right carotid (RC) bifurcation with leftward rotation of the head [7]. In a preliminary study, we have found geometric and hemodynamic changes in the RC bifurcation with a rightward rotation of the head [8]. The objective of this study was, therefore, to investigate the alteration in the geometric parameters of both carotid bifurcations with head posture change by performing morphological MRI studies on healthy volunteers for the normal supine position and the sleeping prone position with head rotation. This has not been previously investigated and is necessary to assess the potential geometric change in the case of the prone sleeping position. This is a customary sleeping posture of many individuals and it may expose the carotids to a geometric change for an extended period of time with unknown pathologic implications. Furthermore, prone position provides the maximum head rotation achievable in an easily reproducible manner.

II. Methods

We defined specific geometric parameters of the carotid bifurcation such as bifurcation angle, internal carotid artery (ICA) angle, asymmetry angle, planarity angle, tortuosity and curvature, and compared their corresponding values in two head postures: 1) the neutral supine position; and 2) the prone position with head rotation to the right (up to 80°).

Manuscript received April 29, 2010; revised October 26, 2010; accepted October 29, 2010. Date of publication November 11, 2010; date of current version January 4, 2011. This work was supported in part by the Foundation of Promotion of Research, Nicosia, Cyprus, under Grant KYSLO/0407/05.

N. Aristokleous is with the Cyprus University of Technology, Limassol 3603, Cyprus (e-mail: n.aristokleous@cut.ac.cy).

I. Seimenis and E. Eracleous are with Ayios Therissos Medical Diagnostic Center, Nicosia 2034, Cyprus (e-mail: yseimen@phys.uoa.gr; elenerac@logosnet.cy.net).

Y. Papaharilaou is with the Institute of Applied and Computational Mathematics, Foundation for Research and Technology - Hellas, Heraklion 700 13, Greece (e-mail: yannisp@iacm.forth.gr).

G. Georgiou is with the University of Cyprus, Nicosia 1678, Cyprus (e-mail: georgios@ucy.ac.cy).

B. C. Brott is with the University of Alabama, Birmingham, AL 35294-1150 USA (e-mail:bbrott@uab.edu).

A. S. Anayiotos is with the Cyprus University of Technology, Limassol 3603, Cyprus, and also with the University of Alabama, Birmingham, AL 35294-1150 USA (e-mail:aanayiot@uab.edu).

Color versions of one or more of the figures in this paper are available online at http://ieeexplore.ieee.org

Digital Object Identifier 10.1109/TITB.2010.2091417

A. Study Group

The group of volunteers consisted of ten asymptomatic and presumably healthy men with no evidence of stenosis or any chronic disease and a mean age of 35± 6 years (range 25–50 years). The study was approved by the Cyprus Bioethics Committee (2006).

B. MRI

MR images were acquired using a 3 T MRI instrument (Philips Healthcare, the Netherlands) at "Ayios Therissos" Medical Diagnostic Center (Nicosia, Cyprus). The built-in quadrature body coil was used for excitation. A phased array head–neck coil and a phased array, flexible, superficial coil were used for signal detection in supine and prone positions, respectively. A series of 100 thin sequential slices were obtained in the axial plane by 3-D time of flight methods, covering the entire left carotid (LC) and RC artery bifurcations and including parts of the common carotid artery (CCA), ICA, and external carotid artery (ECA). A gradient-echo pulse sequence was implemented with an echo time of 2.4 ms and a repetition time of 3.5 ms, while a nominal flip angle of 20° was used. The acquisition voxel size was 0.36 mm × 0.36 mm × 1.2 mm and the reconstructed voxel 0.2 mm × 0.2 mm × 0.6 mm. A parallel imaging technique (SENSE factor 2) was employed to reduce acquisition time. Variable flip angle (16–24°) and gradient first moment nulling techniques were applied to decrease saturation effects of inflowing blood and reduce signal loss due to complex flow, respectively. Each subject was imaged in two different scanning sessions on the same day corresponding to the two head postures examined: 1) a neutral head posture with the subject in the supine position; and 2) a rightward head rotation posture with the subject in the prone position. Two of the subjects were scanned using the same MR protocol on a different day but within a month from the first scan, to allow assessment of the accuracy of the experimental procedure. To examine the effect of contradirectional head rotation, the same two volunteers were, subsequently, scanned in prone position with head rotation to the left.

C. Virtual Model Development

MR images were exported in DICOM format and were converted to a single volume.img format using ImageJ (ImageJ, NIH, U.S.). The solid surface models were constructed by manual segmentation on a slice-by-slice basis (ITK-Snap, Paul Yushkevich, Penn Image Computing and Science Laboratory (PICSL), U.S.) and saved in .stl format [9], [10]. The 3-D geometry of the carotid bifurcation was processed using the vascular modeling toolkit (VMTK) [11]. A smoothing technique from VMTK utilizing the Taubin algorithm [12], which preserves the volume enclosed by the arterial surface, was used for the reconstruction of the 3-D lumen surface.

D. Geometric Feature Quantification

Using various features of the VMTK package, specific important geometric parameters were identified such as bifurcation angle, ICA angle, ICA planarity angle, in-plane asymmetry angle, curvature and tortuosity. The bifurcation area ratio, ICA/CCA, ECA/CCA, and ECA/ICA diameter ratios were also calculated for RCs and LCs. The geometric parameter definitions (see Fig.1) are as follows: bifurcation angle is the angle between the projections of ICA and ECA vectors on to the bifurcation plane. ICA angle is the angle between the projections of CCA and ICA on to the bifurcation plane. ICA planarity angle is the angle between the out of plane components of the CCA and ICA vectors. In-plane asymmetry angle is defined as the difference between two angles, the angle between ICA and CCA and the angle between CCA and ECA. Vessel tortuosity was calculated as $L/D - 1$ where L is the length of the centerline from the origin to the end of the branch, and D is the Euclidean distance between these two points. The vessel curvature is defined as the inverse of the radius of the local osculating circle. Curvature values were averaged over the length of the CCA, ECA, and ICA segments of the computed centerlines. All carotid models were clipped at specific locations (CCA3, ICA5, and ECA5, as shown in Fig. 1) near the bifurcation and, therefore, similar lengths of CCA, ICA, and ECA segments were used for tortuosity and curvature calculations independent of carotid, subject, and scanning session. The bifurcation area ratio was calculated as the sum of the ICA and ECA areas (levels ICA5 and ECA1 in Fig.1) divided by the CCA area (level CCA3 in Fig. 1), ICA/CCA, ECA/CCA, and ECA/ICA diameter ratios were calculated as the square root of the corressponding area ratios [13], equivalent to vessel cross-sectional areas at levels CCA3, ICA5, and ECA1 in Fig. 1.

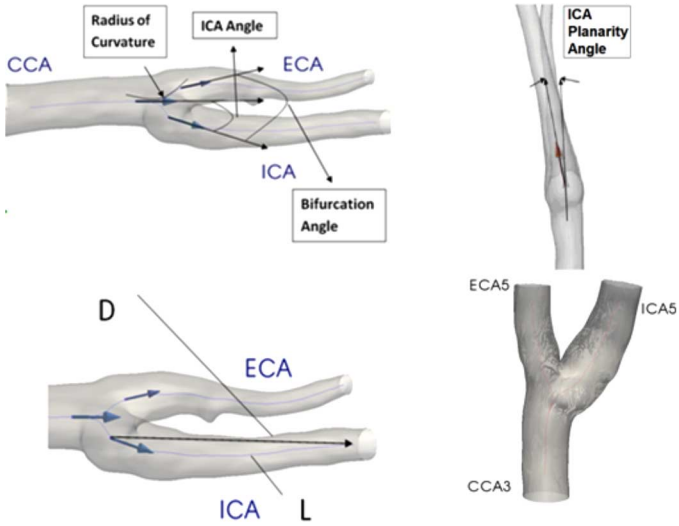

Fig. 1. Graphical representation of some of the bifurcation geometric parameters assessed in this study.

E. Statistical Analysis

Statistical analysis was performed using the open-source R language and environment for statistical computing (version 2.7.2) [14]. Data are presented as median values and interquartile ranges. The Wilcoxon signed-rank test was used for comparisons between the prone and supine positions. For

TABLE I
RESULTS OF THE REPRODUCIBILITY STUDY

	Geometric Parameter		Volunteer I		Volunteer II	
			Right Carotid	Left Carotid	Right Carotid	Left Carotid
			% error in absolute value	% error in absolute value	% error in absolute value	% error in absolute value
Angles	Bifurcation Angle	Supine	0.69	25.00	1.74	11.45
		Prone	23.95	12.15	1.94	15.53
	ICA Angle	Supine	12.89	31.83	7.57	9.25
		Prone	4.63	33.21	16.07	15.60
	ICA Planarity Angle	Supine	97.75	19.52	84.43	273.17
		Prone	46.22	31.01	208.42	53.75
	Asymmetry Angle In Plane	Supine	118.43	49.51	500.00	1.29
		Prone	79.10	9.47	88.85	70.73
Area	Bifurcation Area Ratio	Supine	11.94	0.83	6.00	7.89
		Prone	37.50	17.71	26.45	28.83
	ICA/CCA	Supine	1.32	1.23	2.60	1.18
		Prone	2.44	1.37	12.36	2.47
	ECA/CCA	Supine	10.34	4.05	4.76	9.38
		Prone	37.50	20.00	15.63	28.36
	ECA/ICA	Supine	8.77	6.52	1.22	8.00
		Prone	38.97	22.73	4.17	25.61

comparisons between the LCs and RCs, the Wilcoxon rank sum test (Mann–Whitney test) was used. Statistical correlations for the percentage changes of some of the parameters extracted were evaluated using the Spearman rho correlation coefficient. The value $p < 0.05$ was considered to indicate significance.

F. Reproducibility and Accuracy in Geometric Parameter Extraction

The reproducibility of geometric reconstruction is one of the most crucial steps in the modeling process [15]–[19], and for that reason the accuracy of the segmentation and reconstruction procedures as well as of the geometric parameter estimation was assessed. To assess reproducibility, we repeated 1) the MRI acquisition procedure for two of the volunteers and for both head postures using the same experimental setup and MRI protocol; and 2) the segmentation and solid surface modeling processes.

To optimize the effect of the surface smoothing parameters on the reconstructed solid model, we slightly varied the passband value (from 0.03 to 0.2) and number of iterations (from 15 to 70) for all reconstructed models. Passband is the cut off spatial frequency of the low-pass filter, and the number of iterations is the number of smoothing passes run by VMTK.

III. RESULTS

Table I shows the results of the reproducibility study undertaken to evaluate the accuracy of the geometric parameter extraction. The table indicates the percentage difference (error) in the calculations of each geometric parameter after repeating the whole procedure of data acquisition and postprocessing.

The results demonstrate that, for both volunteers and postures studied, computed values of bifurcation angle and ICA angles, the error is acceptable. For the ICA planarity and asymmetry angles, the error is unacceptable possibly due to the fact that these two angles are calculated by employing space vector, which means that small changes in vector parameters may lead to large angle changes. For the bifurcation area ratio, ICA/CCA, ECA/CCA, and ECA/ICA diameter ratios, tortuosity and curvature, the error is strongly variable, partly due to the limited resolving power of the technique (i.e., short range of measured values). The reproducibility of the geometric parameters for the two extreme cases of 1) passband filter $= 0.03$, iterations $= 15$; and 2) passband filter $= 0.2$, iterations $= 70$ had showed smaller changes than the changes indicated in Table I. Therefore, an optimized passband value of 0.04 and the number of iterations 60 were used on the basis of the closest possible approximation between the volumes of the original, the unsmoothed segmented model and the final reconstructed solid model. Fig. 2 represents reconstructed solid models of both carotid bifurcations for two of the volunteers and for the two head postures studied, i.e., neutral supine and prone with rightward head rotation. The reconstructed models highlight the interindividual variability, the geometric variation between theLCs and RCs, as well as the significant effect that posture change inflicts on vascular geometry. Fig. 3 shows the scatter plots for the bifurcation and ICA angle changes in both carotids. Correlation analysis results showed that, for the RC artery, there was moderate correlation (rho $=$ 0.69) between the percentage changes in bifurcation and ICA angles with head rotation for the ten volunteers studied. For the LC only, the percentage changes for bifurcation angle and ICA angle showed no correlation (rho $= 0.26$). The percentage changes in bifurcation angle for the two carotids also showed no correlation (rho $= 0.07$), as did the percentage changes in ICA between LCs and RCs. Regarding tortuosity and curvature percentage changes, no significant correlations were found for either carotid or between the two vessels. Fig. 4 represents

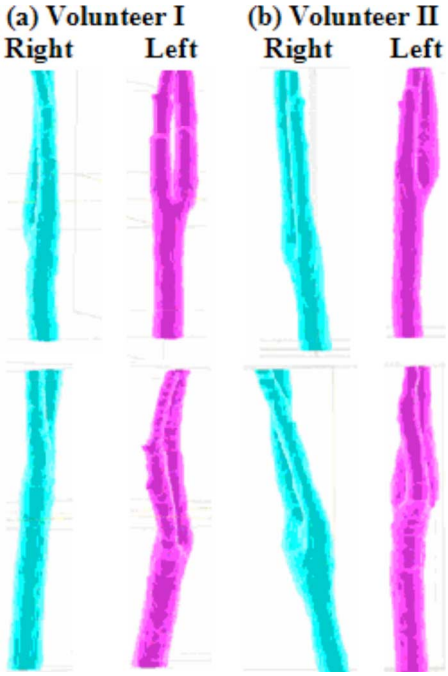

Fig. 2. Reconstructed solid models of both carotid bifurcations for two volunteers and for the two head postures studied.

the differences between supine and prone postures for the bifurcation angle of both carotids and for all volunteers. Fig. 5 shows the differences between supine and prone positions for the ICA angle. It is evident that head rotation to the right affects bifurcation and ICA angles of both carotids. It seems, however, that head rotation alters the ICA angle more than the bifurcation angle in relative values. The results for both angles are in accordance with similar findings from a much larger sample of volunteers [13]. Fig. 6 represents synoptically the median values and interquartile ranges of the geometric parameters estimated from all volunteers. Data are shown for both carotids and head postures. For the RC artery, the bifurcation and ICA angles increase significantly with head rotation to the right, while both angles of the LC decrease in prone position. Median values for tortuosity and curvature do not differentiate substantially with head rotation, while ICA and ECA vessels typically exhibit higher curvature in comparison to CCA independently of head posture. Computed median values of area and diameter ratios also suggest that there is no strong dependence of relative lumen diameter and area on head posture. Comparison beteween the RCs and LCs revealed a significantly ($p = 0.04$) higher bifurcation angle in the supine position, as well as a significantly ($p = 0.04$) lower ICA angle in the prone position, for the left vessel. For both bifuraction angle and ICA angle, head rotation to the left seems to inflict a change toward the same direction (i.e., increase or decrease) as that effected by head rotation to the right, for both carotids.

IV. Discussion

The results of this study confirm previous findings [15]–[19] with regard to the considerable interindividual variability in the geometry of the carotid bifurcations. Presented data also document that there is substantial variability in the geometric features of the LCs and RCs for the same individual.

Our results show that for all volunteers there are significant changes in the geometric parameters of the carotid bifurcation when the head is rotated. This was observed for both the LC and RC bifurcations. These changes are random and there is no predisposition to a specific direction of change for any of the parameters extracted. The variable pattern change demonstrated might be due to the considerable variability observed in the baseline geometry among subjects. Nevertheless, head rotation toward a specific direction can have a different effect on the same geometric feature for the two carotid arteries of the same volunteer. As seen in Figs. 4 and 5, in some individuals head rotation causes divergent effects in the two carotids, while in some subjects a significant variation in one carotid is accompanied by minimal change in the other carotid. The fact that no significant correlation was seen in percentage changes either between different angles of the same bifurcation or between the same angle of the two carotids also predicates the variable effect that head rotation incurs on both the magnitude and the direction of angular change. In most volunteers, the results also show some curvature changes for the CCA as well as for the branches (ICA and ECA). In addition, our findings show that a change in head posture is not associated with a significant alteration in relevant area and diameter ratios, suggesting that any potential alterations in the local flow fields are not due to significant cross-sectional changes.

Vascular compliance varies from individual to individual, and therefore, mechanical stress also presents significant intersubject variations in pattern as well as in magnitude [20]. The variable and frequently significant changes in geometric parameters at the prone position that is a frequent sleeping posture for many subjects and patients could have important consequences in the tensile stress distribution around unstable atherosclerotic plaques. It is believed that atheorosclerotic plaque rupture may be related to maximal mechanical forces at critical sites of high rupture risk. Tang *et al.* [21] have reported that large lipid pools and thin plaque caps are associated with both extreme maximum (stretch) and minimum stress/strain levels. In addition, large cyclic stress/strain variations in the plaque under pulsating pressure were observed that may lead to artery fatigue and possible plaque rupture [22]. This becomes even more important in cases of thin plaque cap and locations with plaque cap weakness that are more closely related to plaque rupture risk [23]. Rotation of the neck structure for a prolonged period that causes changes in bifurcation angle, ICA angle, curvature and tortuosity of the branches may create changes in the stress/strain distribution in plaques susceptible to rupture. So even though this study cannot make claims regarding the susceptibility of plaque rupture in the supine or prone position, the study of unstable plaque morphology and mechanical stress distribution with head rotation are key factors in the plaque rupture process and warrant further investigation [23]. Also, since the disease itself may influence the magnitude and pattern of posture-related geometric alterations, future data should also include geometric changes due to head rotation in the setting of advanced disease.

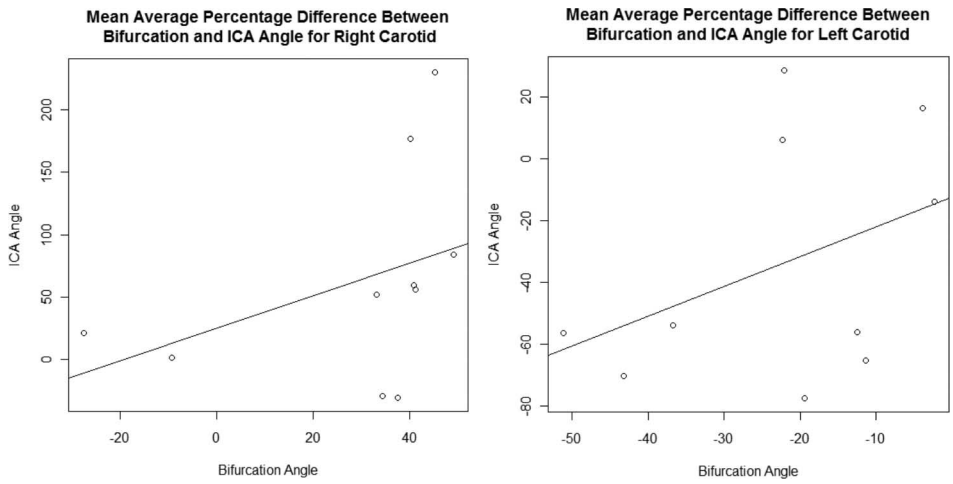

Fig. 3. Scatter plots for correlation values of bifurcation and ICA angle for the right and left carotid.

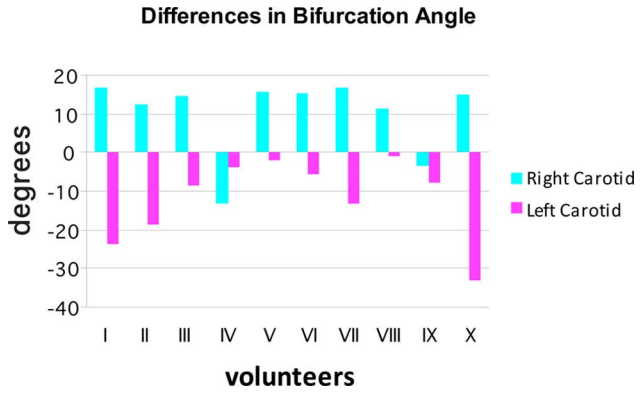

Fig. 4. Differences for the bifurcation angle between neutral and rotation postures of both carotids and for all volunteers. Positive and negative values signify increase and decrease respectively with head rotation.

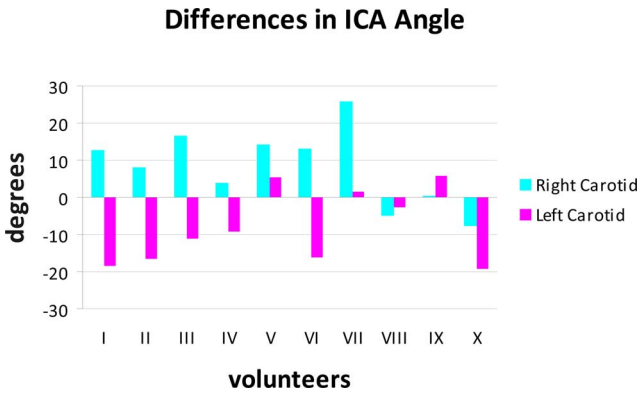

Fig. 5. Differences between neutral and rotation postures for the ICA angle of both carotids and for all volunteers. Positive and negative values signify increase and decrease respectively with head rotation.

Stent implantation in carotid arteries is not common, but it is performed in about 20–30% of patients when endarterectomy is not possible such as in patients with highly calcified lesions or in carotids with complicated geometries [24]. Previous studies such as those by Valibhoy *et al.* [25] and Diehm *et al.* [26] have reported that carotid stents fracture in some occasions. Further research is, therefore, required to investigate the conditions under which stents fracture if the altered geometry of the carotid in the prone/rotated head posture will exacerbate the possibility of fracture. The interindividual variability in the geometry of the carotid artery bifurcation is coupled with a significant variation in arterial flow and mechanical stress patterns among healthy humans [20]. Additionally, Lee *et al.* [27] have demonstrated that there are wide interindividual variations in exposure to the so-called disturbed flow that may be potentially related to atherogenic risk. In this respect, it may be assumed that the carotid geometric changes with the head posture may also impose significant changes in blood dynamics, mechanical stress distributions, and disturbed flow fields. Zhang *et al.* [6] and Lee *et al.* [27] have reported that ICA and CCA tortuosity, curvature and area ratio of ICA to ECA are important parameters in the hemodymamic disturbance level and formation of low/oscillating WSS regions at the carotid bulb. Arterial regions where atheromatous plaques usually develop have been found to be simultaneously exposed to low WSS and high mechanical stress [20]. Our earlier studies [8] indicate that small changes in geometric parameters with head rotation cause changes in hemodynamic parameters that considered to be important in the development of arterial disease such as normalized oscillating shear index and WSS (TG). The effects of such changes to the flow and mechanical fields in the carotid bulb and the development of carotid disease are unknown [28], [29] and need to be clarified.

The number of individuals included in the present study is small and a larger number is required for statistically significant results. The observed large dispersion of the results warrants the examination of a large cohort in order to disambiguate if there are definite trends in the change of bifurcation geometric parameters with posture alteration. In addition, the fact that a fixation system was not possible to be used during the scanning procedure has led to a varying degree of head rotation, thus contributing to a possible large dispersion of acquired results.

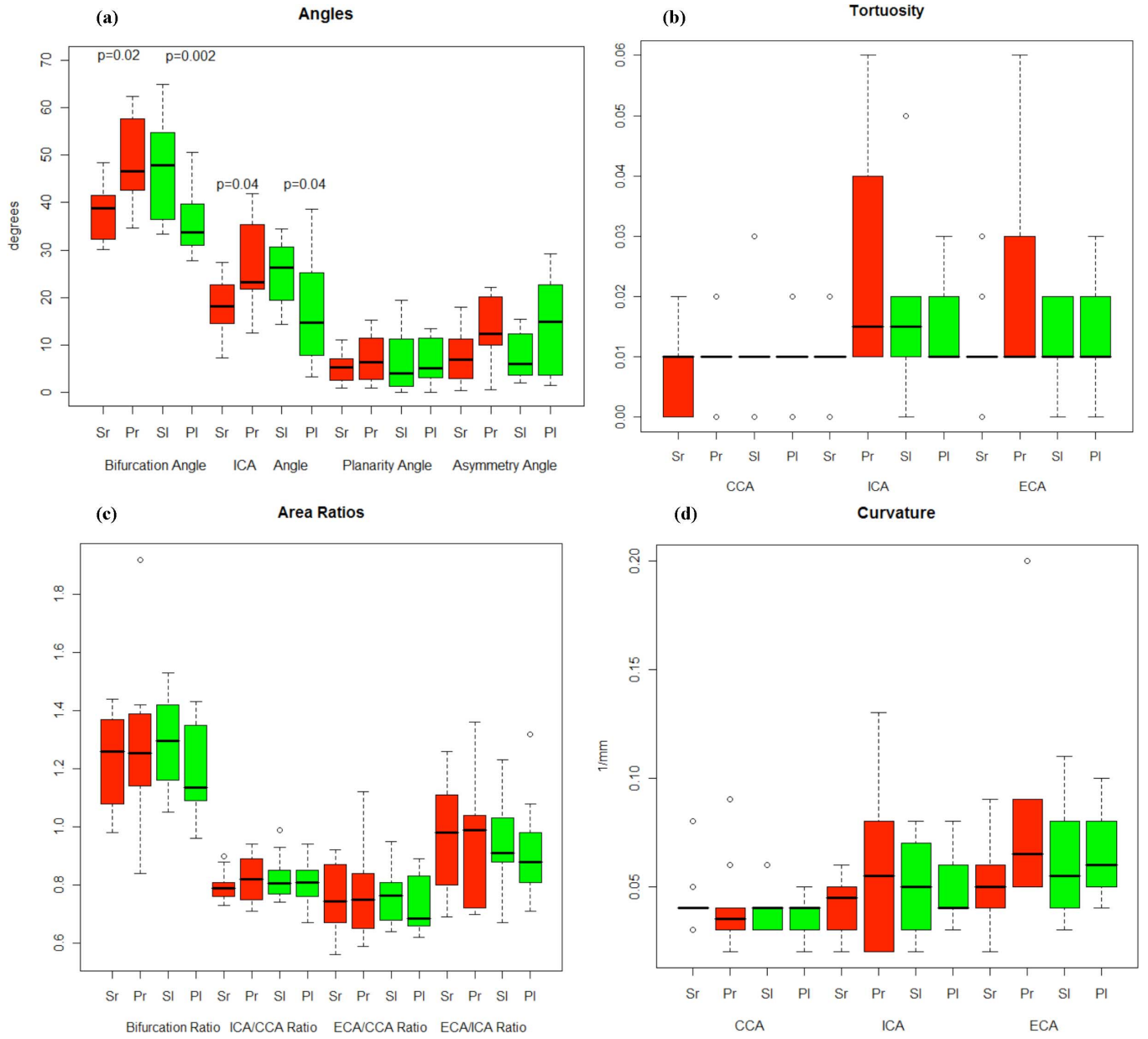

Fig. 6. Box plots showing the median values horizontal line and interquartile ranges (IQR) of the geometric parameters estimated. Dashed lines connect the nearest observations within 1.5 of the IQR of the lower and upper quartiles. Unfilled circles indicate possible outliers with values beyond the ends of the 1.5× IGR. Data are shown for both right (red, r) and left (green, l) carotids in supine (S) and prone (P) head postures. $p < 0.05$ values in the Wilcoxon signed-rank test between the two head postures are also shown.

V. Conclusion

Despite the reduced accuracy in the calculation of some of the geometric parameters studied, the results of the present study suggest that head rotation may cause significant variation in bifurcation angle, ICA angle, planarity angle, and asymmetry angle, as well as in vessel tortuosity and curvature. It seems, however, that these changes are random and depend on the geometry and elasticity of the whole neck arterial tree and there is no consistency regarding the direction and extent of change. The significant geometric variations with posture change observed in most of the volunteers studied, warrant 1) a thorough investigation of the geometry of unstable plaque in atherosclerotic patients and the possible changes in the distribution of mechanical stress with head rotation; 2) an investigation of the vascular morphology of stented arteries with head rotation; and 3) an investigation of the hemodynamics of the carotid with head rotation and particularly the hemodynamic parameters related to the development of atherosclerotic disease, such as low oscillating WSS and particle residence times.

References

[1] D. Lloyd-Jones, R. J. Adams, T. M. Brown, M. Carnethon, S. Dai, G. De Simone, T. B. Ferguson, E. Ford. K. Furie, C. Gillespie, A. Go, K. Greenlund, N. Haase, S. Hailpern, P.M. Ho, V. Howard, B. Kissela, S.

Kittner, D. Lackland, L. Lisabeth, A. Marelli, M. M. McDermott, J. Meigs, D. Moyaffarian, M. Mussolino, G. Nichol, V. Roger, W. Rosamond, R. Sacco, P. Sorlie, R. Stafford, T. Thom, S. Wasserthiel-Smoller, N. D. Wong, and J. Wylie-Rosett, "Heart disease and stroke statistics—2010 update: A report from the American Heart Association," *Circulation*, vol. 121, pp. e46–e215, 2010.

[2] R. A. White, G. A. Sicard, R. M. Zwolak, A. N. Sidawy, M. L. Schermerhorn, R. J. Shackelton, and F. S. Siami, "Society of vascular surgery vascular registry comparison of carotid artery outcomes for atherosclerotic vs nonatherosclerotic carotid artery disease," *J. Vasc. Surg.*, vol. 51, no. 5, pp. 1116–1123, 2010.

[3] M. Fisher and S. Fieman, "Geometric factors of the bifurcation in carotid atherogenesis," *Stroke*, vol. 21, pp. 267–271, 1990.

[4] U. G. R. Schulz and P. M. Rothwell, "Major variation in carotid bifurcation anatomy. A possible risk factor for plaque development?," *Stroke*, vol. 32, pp. 2522–2529, 2001.

[5] D. R. Wells, J. P. Archie, and C. Kleinstreuer, "Effect of carotid artery geometry on the magnitude and distribution of wall shear stress gradients," *J. Vasc. Surg.*, vol. 23, pp. 667–678, 1996.

[6] M. H. Friedman, O. J. Deters, F. F. Mark, C. B. Bargeron, and G. M. Hutchins, "Arterial geometry affects hemodynamics," *Atherosclerosis*, vol. 46, pp. 225–231, 1983.

[7] F. P. Glor, B. Ariff, A. D. Hughes, P. R. Verdonck, D. C. Barratt, A. D. Augst, S. A. M. Thom, and X. Y. Xu, "Influence of head position on carotid hemodynamics in young adults," *Am. J. Physiol. Heart Circ. Physiol.*, vol. 287, pp. 1670–1681, 2004.

[8] Y. Papaharilaou, Y. Seimenis, N. Pattakos, J. Ekaterinaris, G. Georgiou, E. Eracleous, C. Christou, B. Brott, and A. S. Anayiotos, "Effect of head posture changes in the geometry and hemodynamics of a healthy human carotid bifurcation," presented at the ASME 2007 Summer Bioengineering Conf. (SBC), Keystone Resort & Conference Center, Keystone, CO, Jun. 20–24.

[9] P. A. Yushkevich, J. Piven, H. C. Hazlett, R. G. Smith, S. Ho, J. C. Gee, and G. Gerig, "User-guided 3D active contour segmentation of anatomical structures: Significantly improved efficiency and reliability," *Neuroimage*, vol. 31, pp. 1116–1128, 2006.

[10] T. Hassan, E. V. Timofeev, T. Saito, H. Shimizu, M. Ezura, T. Tominaga, A. Takahashi, and K. Takayama, "Computational replicas: Anatomic reconstructions of cerebral vessels as volume numerical grids at three-dimensional angiography," *Am. J. Neuroradiol.*, vol. 25, pp. 1356–1365, 2004.

[11] L. Antiga and D. A. Steimman, "Robust and objective decomposition and mapping of bifurcating vessels," *IEEE Trans. Med. Imaging*, vol. 23, no. 6, pp. 704–713, Jun. 2004.

[12] G. Toubin, "A signal processing approach to fair surface design," in *Proc. SIGGRAPH Conf.*, 1995, pp. 351–358.

[13] J. B. Thomas, L. Antiga, S. L. Che, J. S. Milner, D. A. H. Steinman, J. D. Spence, B. K. Rutt, and D. A. Steinman, "Variation in the carotid bifurcation geometry of young versus older adults: Implications for geometric risk of atherosclerosis," *Stroke*, vol. 36, pp. 2450–2456, 2005.

[14] R Development Core Team (2008), [Online]. Available: http://www.R-project.org

[15] Q. Long, B. Ariff, S. Z. Zhao, S. A. Thom, A. D. Hughes, and X. Y. Xu, "Reproducibility study of 3D geometrical reconstruction of the human carotid bifurcation from magnetic resonance images," *Magn. Reson. Med.*, vol. 49, no. 4, pp. 665–674, 2003.

[16] J. B. Thomas, J. S. Milner, B. K. Rutt, and D. A. Steinman, "Reproducibility of image-based computational fluid dynamics models of the human carotid bifurcation," *Ann. Biomed. Eng.*, vol. 31, no. 2, pp. 132–141, 2003.

[17] J. A. Moore, D. A. Stenman, D. W. Holdsworth, and C. R. Ethier, "Accuracy of computational hemodynamics in complex arterial geometries reconstructed from magnetic resonance imaging," *Ann. Biomed. Eng.*, vol. 27, no. 1, pp. 32–41, 1999.

[18] D. A. Steinman, "Image-based computational fluid dynamics modeling in realistic arterial geometries," *Ann. Biomed. Eng.*, vol. 30, no. 4, pp. 483–497, 2002.

[19] F. P. Glor, B. Ariff, L. A. Crowe, A. D. Hughes, P. L. Cheong, S. A. McG. Thom, P. R. Verdonck, D. N. Firmin, D. C. Barratt, and X. Y. Xu, "Carotid geometry reconstruction: A comparison between MRI and ultrasound," *Med. Phys.*, vol. 30, no. 12, pp. 3251–3261, 2003.

[20] S. Z. Zhao, B. Arifff, Q. Long, A. D. Hughes, S. A. Thom, A. V. Stantom, and X. Y. Xu, "Inter-individual variations in wall shear stress and mechanical stress distributions at the carotid artery bifurcation of healthy humans," *J. Biomech.*, vol. 35, pp. 1367–1377, 2002.

[21] D. Tang, C. Yang, J. Zheng, P. K. Woodard, J. E. Saffitz, J. D. Petruccelli, G. A. Sicard, and C. Yuan, "Local maximal stress hypothesis and computational plaque vulnerability index for atherosclerotic plaque assessment," *Ann. Biomed. Eng.*, vol. 33, no. 12, pp. 1789–1801, 2005.

[22] D. Tang, C. Yang, J. Zheng, P. K. Woodard, G. A. Sicard, J. E. Saffitz, and C. Yuan, "3D MRI-based multicomponent FSI models for atherosclerotic plaques," *Ann. Biomed. Eng.*, vol. 32, no. 7, pp. 947–960, 2004.

[23] C. Yang, R. G. Bach, J. Zheng, I. Ei Naqa, P. K. Woodard, Z. Teng, K. Billiar, and D. Tang, "*In vivo* IVUS-based 3-D fluid-structure interaction models with cyclic bending and anisotropic vessel properties for human atherosclerotic coronary plaque mechanical analysis," *IEEE Trans. Biomed. Eng.*, vol. 56, no. 10, pp. 2420–242, Oct. 2009.

[24] A. W. F. Vos, M. A. M. Linsen, J. T. Marcus, J. C. Van Den Berg, J. A. Vos, J. A. Rauwerda, and W. Wisselink, "Carotid artery dynamics during head movements: A reason for concern with regard to carotid stending?," *J. Endovasc. Ther.*, vol. 10, pp. 862–869, 2003.

[25] R. Valibhoy, B. P. Mwipatayi, and K. Sieunarine, "Fracture of a carotid stent: An unexpected complication," *J. Vasc. Surg.*, vol. 45, pp. 603–606, 2007.

[26] N. Diehm, S. Baum, B. Katzen, M. Kovacs, and J. Benenatiref, "Fracture of a carotid stent: A word of caution," *J. Vasc. Int. Radiol.*, vol. 19, no. 4, pp. 622–623, 2008.

[27] S. W. Lee, L. Antiga, J. D. Spence, and D. A. Steinman, "Geometry of the carotid bifurcation predicts its exposure to disturbed flow," *Stroke*, vol. 39, pp. 2341–2347, 2008.

[28] I. Marshall, S. Zhao, P. Papathanasopoulou, P. Hoskins, and X. Y. Xu, "MRI and CFD studies of pulsatile flow in healthy and stenosed carotid bifurcation models," *J. Biomech.*, vol. 37, no. 5, pp. 679–687, 2004.

[29] N. Ku, D. P. Giddens, C. K. Zarins, and S. Glagov, "Pulsatile flow and atherosclerosis in the human carotid bifurcation. Positive correlation between plaque location and low oscillating shear stress," *Arteriosclerosis Thrombosis Vascular Biol*, vol. 5, pp. 293–302, 1985.

Author's photograph and biographies not available at the time of publication.